Importance of Surface Coating to Accumulation Dynamics and Acute Toxicity of Copper Nanomaterials and Dissolved Copper in Daphnia magna

Zuzanna Gajda-Meissner ORCID iD: 0000-0002-3278-9160

19-00105

Environmental Chemistry

Gajda-Meissner et al.

Running Head: Importance of surface coating on accumulation dynamics

Importance of Surface Coating on Accumulation Dynamics and Acute Toxicity of Copper Nanomaterials and Dissolved Copper to *Daphnia magna*

Zuzanna Gajda-Meissner[*], Konrad Matyja[*], David Brown[¥], Mark G. J. Hartl[§], Teresa F. Fernandes[§]

*Heriot-Watt University, School of Energy, Geoscience, Infrastructure and Society, Institute of Life and Earth Sciences, Centre for Marine Biodiversity & Biotechnology, Edinburgh

[*]Wroclaw University of Science and Technology, Faculty of Chemistry, Division of Bioprocess and Biomedical Engineering, Wrocław, Poland

[¥]Heriot-Watt University, School of School of Engineering and Physical Sciences, Institute of Biological Chemistry, Biophysics and Bioengineering, Edinburgh

(Submitted 15 February 2019; Returned for Revision 05 April 2019; Accepted 10 October 2019)

Abstract: In this study the effect of copper oxide nanomaterials (CuO NMs), uncoated and with three different surface coatings (i.e. carboxylated, pegylated and ammonia

groups), was evaluated on acute toxicity and accumulation dynamics in *Daphnia magna*. Biosorption and elimination rate constants were determined for *D. magna* following waterborne exposure to dissolved copper and copper oxide NMs using biodynamic modeling. The relationship between modeled parameters and acute toxicity endpoints was evaluated to investigate if accumulation dynamics parameters could be used as a predictor of acute toxicity. The Langmuir equation was used to characterize the biosorption dynamics of copper NMs and copper chloride, used as dissolved copper control. Uptake rates showed the following ranking: pristine-CuO NMs > NH_3-CuO NMs > aqueous Cu > PEG-CuO NMs > COOH-CuO NMs. To determine copper elimination by *D. magna* a one compartment model was used. Different elimination rate constants were estimated for each chemical substance tested. Those which were easily biosorbed were also easily removed from organisms. Biosorption and depuration properties of NMs were correlated with zeta potential values and diameter of NMs agglomerates in the suspensions. There is no link between biosorption and toxicity. Waterborne exposures to more difficult to biosorb CuO NMs are likely to induce adverse effects more than those which are easily to biosorb. It is proposed that some physicochemical properties of NMs in media, including zeta potential and agglomerate diameter, can lead to higher biosorption but do not necessarily affect toxicity. The mode of interaction of the NMs with the organism, seems to be complex and depends on chemical speciation and physicochemical properties of NMs inside an organism. Moreover our findings highlight that coating type affects the biosorption dynamics, depuration kinetics and dissolution rate of NMs in media.

Keywords: copper, dose-response modeling, metal uptake

This article includes online-only Supplemental Data.

*Address correspondence to z.gajda-meissner@hw.ac.uk

Published online XXXX 2019 in Wiley Online Library (www.wileyonlinelibrary.com).

DOI: 10.1002/etc.xxxx

Graphical Abstract

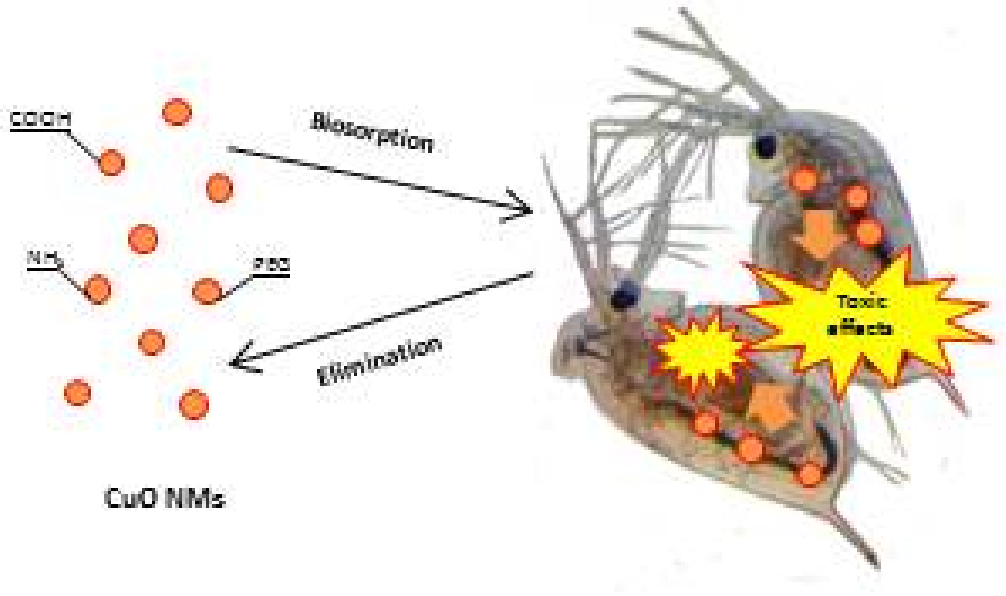

INTRODUCTION

Copper oxide nanomaterials (CuO NMs) are widely used as an efficient antibacterial agent in paints (Palza et al. 2018), and in many biological applications combating a range of bacterial pathogens, including meticillin-resistant *Staphylococcus aureus* (MRSA) and *Escherichia coli* (Ren et al. 2009). CuO NMs are also frequently used in commercial products, such as biosensors or electrochemical sensors and their production continues to increase to meet demand (Xu et al. 2018). Consequently, there is concern about the safety of NMs and therefore understanding and predicting their environmental impact has become an issue of great importance (Cohen et al. 2013; Winkler 2016). Due to the rapid expansion of nanotechnology and the increasing range of NMs under production and development, it is essential that the potential impacts on human and environmental health are addressed. Among the emerging literature concerned with the biological effects of NMs, there is still a lack of information (Nolte et al. 2017), particularly regarding the hazards related to the surface modifications of NMs towards organisms in the environment. CuO NMs may constitute an environmental hazard because of the high toxicity of copper to aquatic species (Kahru and Dubourguier 2010). Jo et al. (2012) demonstrated that CuO NMs and silver NMs (Ag NMs) are toxic to *D. magna* through (mostly) the dissolved fraction in the water column. In addition, they demonstrated that

the method of dispersion affected the toxicity of CuO and Ag NMs. Also, Aruoja et al. (2008) reported that CuO and ZnO NMs were toxic to *Raphidocelis subcapitata* at very low concentrations. The 72h EC_{50} values of ZnO and CuO NMs reported by these authors were 0.042 mg L^{-1} and 0.71 mg L^{-1}. Heinlaan et al. (2011) determined time-dependent changes in *D. magna* midgut epithelial ultrastructure after exposure to CuO NMs. Several studies have evaluated the toxicity of various NMs to different aquatic species. Heinlaan et al. (2011) investigated the effect of ZnO, CuO and TiO_2 NMs to the bacteria *Vibrio fisheri* and crustaceans *D. magna* and *Thamnocephalus platyurus*, using a combination of traditional ecotoxicology assays and metal-specific recombinant biosensor recombinant *E. coli* to determine the toxicity pathway of ZnO and CuO NMs, as well as the toxicity attributed to the solubilized ionic fractions of zinc and copper. They quantified bioavailable metal ions using recombinant metal sensor bacteria in which bioluminescence is induced by intracellular metal ions. The induction is mediated by a specific protein that recognizes the respective metal ion and regulates a promoter controlling the expression of luxCDABE genes leading to bioluminescence. The toxicity ranking of metal oxides NMs to *V.fisheri* was as follows: TiO_2 < CuO < ZnO. The 30 min EC_{50} values for TiO_2, CuO and ZnO were <20000 mg L^{-1}, 3811 mg L^{-1} and 1.8 mg L^{-1}, respectively. The same toxicity pattern was observed towards the crustaceans *D. magna and T. platyurus*. The toxicity ranking of metal oxides NMs to *D. magna* was as follows: TiO_2 < CuO < ZnO. The 48h EC_{50} values for TiO_2, CuO and ZnO were <20000 mg L^{-1}, 3.2 mg L^{-1} and 3.2 mg L^{-1}, respectively (Heinlaan et al. 2011). The toxicity ranking of metal oxides NMs to *T. platyrus* was as follows: TiO_2 < CuO < ZnO. The 48h EC_{50} values for TiO_2, CuO and ZnO were <20000 mg L^{-1}, 1.65 mg L^{-1} and 0.18 mg L^{-1} respectively. Among the tested crustaceans *T. platyurus* was the most sensitive species, with the 48h EC_{50} values for TiO_2, CuO and ZnO being 20000 mg L^{-1}, 1.65 mg L^{-1} and 0.12 mg L^{-1} respectively (Heinlaan et al. 2011).

Modifications of NMs for different applications can change their physicochemical properties such as surface charge, size, biosorption and depuration properties, and influence their toxicity (Chen and Mao 2007). The fate and behaviour of NMs can be modulated by various types of coatings which may affect their uptake by organisms, their mode of binding to different structures of a living organism and their release of soluble

metals (Liu et al. 2010). Assessments of the extent to which such modifications influence the acute toxicity of NMs, biosorption and elimination behaviors are needed to understand the potential environmental risks these modified NMs may pose, and also to assess if certain modifications may mitigate toxicity. Assessment of the role of various NM's surface modifications on their effects on *D. magna* was thus the main aim of the present study. In this work the focus was the assessment of the effects of each NM (and metal salt) taking into consideration toxicity of the metal fraction in each treatment. In parallel biosorption was also assessed. The reasoning for this was to allow the assessment of biosorption, and if, and how, this could be related to toxicity. In this work biosorption is defined as a physicochemical removal process of e.g. metal and metalloid compounds from solution by biological material (Gadd 1990; Wang and Chen 2009). The biosorption process is based on the following metabolism dependent and independent mechanisms: adsorption, absorption, ion exchange, precipitation, surface complexation and transmembrane transport processes (Veglio and Beolchini 1997; Wang and Chen 2009; Fomina and Gadd 2014). These processes can lead to accumulation of materials onto the surface of organisms as well as within. In the case of relatively large organisms, like *D. magna*, additional processes which can affect the parameters of observed biosorption should be indicated – e.g. actively looking for food, active food intake and uptake of NMs associated with the food. However, it is assumed that the bioaccumulation process can be described by commonly used biosorption models (Wang and Chen 2009). Furthermore, during acute toxicity tests daphnids are not fed. Therefore, in the present study the term biosorption is used instead of bioaccumulation. Frequently used biosorption models are the Langmuir and Freundlich isotherms (Wang and Chen 2009). They both describe the relationship between the amount of sorbed material and the concentration of this material in solution at equilibrium. To describe the kinetic of changes which occur before equilibrium is reached the first-order Lagergren model, or the pseudo-second-order equation, can be used (Wang and Chen 2009). The usage of Langmuir and Lagergren models in toxicity assessment is demonstrated in this study. The relationship, if any, between estimated parameters of these models and dose-response curve parameters obtained from acute tests was assessed and discussed.

MATERIALS AND METHODS

Experimental design

D. magna cultures

D. magna used in this study are part of a culture kept at Heriot-Watt University. The culture medium was renewed twice a week and daphnids were fed daily with algae (*Chlorella vulgaris*). The culture was maintained at a constant temperature (21 ± 1ºC) with 8:16 hours light-dark cycle.

Medium

M7 medium was prepared according to OECD guideline 202 (without EDTA).

Copper chloride and NMs

Four different NMs were used. Unmodified pristine CuO and CuO NMs functionalized with COOH, NH_3 and PEG (polyethylenegycol) groups. All CuO NMs were provided by PlasmaChem with particles nominal size of 15 nm. Copper chloride ($CuCl_2$) was obtained from Sigma-Aldrich (purity > 99%).

Characterization of CuO NMs

A stock suspension of 100 µg L^{-1} CuO NMs was prepared by dispersing the NMs in M7 medium in a bath sonicator for 13.6 min (NANOSOLUTIONS Project Standard operating procedure: Dispersion protocol for CuO engineered nanomaterials Ver. 1.0; 2014-02-18). The bath sonicator method used delivers 13 Watts of acoustic power (P_{ac}) to a sample of 100 ml for 13.6 minutes. The samples were analysed immediately after preparation of the NM suspensions. Particle size distributions and zeta potential of these NM suspensions were determined using dynamic light scattering (DLS, Malvern, Zetasizer). Primary particle size was determined by transmission electron light microscopy (TEM).

Zeta potential of D.magna in M7 medium

Zeta potential of *D.magna* in M7 medium was determined using DLS. Five animals were transferred into zeta potential measurements cuvette and samples were analysed immediately.

Dissolution

The soluble fraction of the CuO NMs suspensions was determined by ultracentrifugation (Jiang et al. 2015). Dissolution in the absence of organisms was determined by suspending CuO NMs in M7 medium. Three replicate 10 ml volumes from each sample were pipetted into polycarbonate centrifuge tubes, and spun at 25000 RPM for 1 hour at 20˚C. The dissolved metal was defined as the amount present in the supernatants of the centrifuged samples after digestion in nitric acid (2% HNO_3). Metal concentrations were measured by inductively coupled plasma mass spectrometry (ICP-MS). Three repetitions were measured per sample, and the average was used to calculate the metal concentration.

Biosorption in equilibrium and kinetics elimination experiments

Nonrenewal acute toxicity tests of NMs were conducted following the OECD standard guideline 202 (OECD, 2004) using the M7 medium for 48 hours. Uptake and elimination experiments were based on the concentration ranges determined in preliminary toxicity tests: *D.magna* were exposed for 24 h to 1-15µg l^{-1} copper chloride, 2.5-100µg l^{-1} CuO, and 5-50µg l^{-1} modified copper oxide NMs, respectively. The highest concentration used in this study corresponds to EC_{30} values after 24 hours of exposure. Twenty animals were exposed with three replicates at each exposure, after which *D.magna* were rinsed with Milli-Q grade water to remove externally bound copper particles. Samples were collected into pre-weighed 15 ml Falcon tubes and sacrificed by freezing (Khan et al. 2015).

A second experiment was designed to determine metal uptake and elimination. Briefly, animals were exposed for 24 hours to 15µg l^{-1} copper chloride, 100µg l^{-1} CuO and 30µg l^{-1} modified CuO NMs, respectively. The highest concentration used in this study corresponds to EC_{30} values after 24 hours of exposure. After 24 hours of exposure,

animals were rinsed in fresh medium and transferred to new exposure beakers containing a clean medium for depuration. Twenty individual *D. magna* were collected at each sampling time point (t = 1, 2, 6, 24, 48, 72 and 144 hours post exposure) (Kalman et al. 2015).

In order to assess copper content within the organisms (body burden of copper in daphnids), sampled daphnids from the uptake and elimination experiments were treated following a modified method of Pane et al. (2004). Briefly, animals were thoroughly washed with Mili-Q grade water and then dried to constant weight in an oven at 60°C overnight. The dried samples were digested using pure HNO_3 at 60°C for 2h in a glass beaker. After cooling, the digestate was transferred quantitatively to a 10 mL volumetric flask containing Mili-Q water to obtain a final concentration of HNO_3 2% v/v. The copper amount was determined using ICP-MS.

Additionally, control samples were exposed without copper for 24 hours to ensure that there was no contamination from experimental conditions. *D. magna* were sacrificed to measure the initial background copper (Cu) burden. Background amount of Cu was not subtracted from the measured Cu amount. Instead, background amount was incorporated in the model via estimates from the Langmuir and kinetic models (see explanation below).

Modeling

The mass fraction of copper in NMs

The mass of NMs in each sample was expressed as mass of Cu and calculated using calibration curves prepared separately for each NM type. Nominal concentrations of NMs were added to distilled water. Total Cu concentration was measured using ICP-OES. Results were plotted and a straight line passing through the point (0,0) was fitted to the data using the least squares method. The calibration equation can be expressed as:

$$C_{ex} = mC_{nano} \quad (1)$$

Where: C_{nano} – is the nominal concentration of NMs [µg l^{-1}], C_{ex} – external concentration expressed as a concentration of Cu per volume of culture medium [µg l^{-1}], m – is the coefficient of proportionality (slope of best fit line).

Biosorption in equilibrium

A Langmuir equation was used to model the biosorption of Cu in equilibrium (Wang and Chen 2009). This is the most commonly used model which describes the relationship between the external concentration C_{ex} [µg l^{-1}] of Cu in solution and the amount of biosorbed Cu- C_{in} [µg g^{-1}]. It can be expressed as:

$$C_{in} = \frac{aC_{ex}}{b+C_{ex}} + c_b \quad (2)$$

where: a – is the maximum capacity of Cu in a solid mass of the daphnids' bodies [µg g^{-1}]; b – is an external concentration when C_{in} is equal to 0.5 of a [µg l^{-1}], and c_b - is the background amount of Cu in daphnids [µg g^{-1}].

Kinetics of elimination

A one-compartment model was used to describe the kinetics of Cu associated with the different chemicals tested. Description of uptake and elimination of Cu can be described by the following differential equation which represents the Lagergren model (Wang and Chen 2009):

$$\frac{dC_{in}}{dt} = k_e\left(\frac{k_{up}}{k_e}C_{ex} - C_{in}\right) = k_{up}C_{ex} - k_eC_{in} \quad (3)$$

where: C_{in} – is the amount of Cu biosorbed by the organism [µg g^{-1}]; C_{ex} – external Cu concentration [µg l^{-1}]; k_e – is an elimination constant [h^{-1}]; k_{up} – is an uptake constant [l h^{-1} g^{-1}].

With the assumption that the external concentration in the medium does not change during the elimination of Cu from the organisms' bodies the differential equation can be solved analytically. The assumption is appropriate for relatively large volumes of

the external solution – which meets experimental conditions. A solution of equation (3) for C_{ex} = const. is:

$$C_{in}(t) = C_{in0}e^{-k_e t} + c_b \qquad (4)$$

where: C_{in0} – is the amount of Cu biosorbed by the organism at time 0 [µg g^{-1}]; k_e – elimination rate constant [h^{-1}]; c_b – is the background amount of Cu in daphnids [µg g^{-1}].

The biosorption in equilibrium kinetics of elimination were prepared for total Cu doses. However, CuO NMs dissolved in M7 medium and created mixtures which contained dissolved Cu and Cu in particulateform (NMs). Therefore, it is impossible to determine biosorption and elimination parameters directly for particulate Cu forms, instead the parameters were estimated from the mixture of different Cu forms.

NMs amount adsorbed per unit mass of *D.magna* was the equilibrium concentration of dissolved Cu and particulate Cu in the solution. Elimination experiments were performed to quantify the efflux of dissolved Cu and particulate Cu accumulated in tissue after waterborne exposure. In both experiments dissolved Cu and particulate Cu values were used as an input parameters in modelling the uptake dynamics and depuration kinetic.

Dose-response curves

The log-logistic model was fitted to dose-response data:

$$E(C_{in}) = 1 - \frac{-d + 1}{1 + \left(\frac{C_{in}}{e}\right)^n}$$

where: E – is a toxic effect, here mortality; C_{in} – is the total amount of Cu biosorbed (dissolved plus particulate form) by the organism [µg g^{-1}]; d – is the lowest limit of effect (fitted), the highest limit is fixed at 1 (due to mortality); n – describes the slope of the dose-response curve; e – is the inflection point of the function (when d = 0 e = ED_{50} – the dose which causes 50% effect, here mortality) [µg g^{-1}].

It should be noted that the dose-response curves parameters are actually estimated for both Cu forms (dissolved plus particulate form).

Estimation of models parameters

The estimation of the parameter values for the mentioned models was conducted in Matlab using the nonlinear least squares method. The goodness of fit was characterized by the sum of squared errors (SSE), coefficient of determination (R^2); adjusted coefficient of determination (Adj. R^2 - more useful for comparing models with a different number of predictors) and root mean squared error (RMSE).

RESULTS AND DISCUSSION

Characterization of CuO NMs

The charge and size of the NMs studied can be an important feature affecting their biosorption. Zeta potential can be understood as a potential difference between a point in an interfacial double layer of NMs and the point in the bulk of medium solution that will use a certain amount of energy per charge that passes through these two points (Bhattacharjee 2016). Therefore the zeta value can differ between NMs in different suspensions. It can reflect the mobility of particles and can affect the rate of biosorption (Fröhlich 2012). In this study the zeta potential values obtained for the different NMs suspensions in M7 medium were compared. Zeta potential values, mean value of agglomerate diameter (z-Average), polydispersity index (PDI) and dissolution rate for different types of CuO NMs are shown in Table 1.

The fraction of dissolved Cu in M7 medium for Pristine-CuO NMs was equal to 5% (Table 1). This value is close to those which can be found in the literature (e.g. Misra et al. 2012). Coated NMs seem to be more susceptible to dissolution. The dissolved Cu fraction reached the values of 0.85 and 0.86 in the case of COOH-CuO and PEG-CuO NMs, respectively (Table 1). The dissolved and particulate forms of Cu can contribute to biosorption, elimination and toxicity in various ways (Croteau et al. 2014; Jiang et al. 2017). The behaviour and biosorption of CuO NMs and metal ions released from CuO NMs and $CuCl_2$ in media depended upon the characteristic of coated CuO NMs and Cu

salt. High solubility of COOH-CuO, PEG-CuO and $CuCl_2$ in media was observed however parameters describing biosorption and elimination processes varied significantly across tested CuO NMs and $CuCl_2$. This study demonstrated small contributions of dissolved Cu to overall Cu uptake rates and hence Cu biosorption was mainly dependent upon the percentage of CuO NMs in particulate form.

Primary particle size determined by transmission electron microscopy (TEM) and other physico-chemical properties of CuO NMs are given in Supporting Information (Figure S2 and table S1).

Another important feature of NMs is the mass fraction of copper in a unit of general mass of the certain type of NMs, as described below.

The mass fraction of copper in NMs The calibration curves were prepared to determine the mass fraction of metal in NMs and Cu salt. The *m* parameter (Table 2, Figure S1) was used to calculate the NMs concentrations from the corresponding measured copper concentrations. This transformation was needed to compare the results obtained for the different chemicals tested. Furthermore, it is possible that the metal fraction drives the observed toxicity. This would possibly depend on the chemical speciation of the Cu (Santore et al. 2001; Di Toro et al. 2001).

The highest proportion between Cu and NMs concentration was observed for the pristine-CuO NMs (0.7133) (Table 2). The other NMs showed lower proportions (COOH, NH_3, PEG). The mass fraction of Cu ions in $CuCl_2$ was 0.386 and it was lower than the mass fractions calculated for all NMs apart from PEG-CuO NMs.

Biosorption in equilibrium

The fit of the Langmuir model to the experimental data is presented in Figure 1, and estimated parameter values are listed in Table 3. The Langmuir equation is commonly used to model biosorption processes by different species including: cadmium biosorption on *D. magna* and *C. dubia* (Robinson et al. 2003), chitin and arthropod carapaces(Benguella and Benaissa 2002), cadmium and other metal ions by algae (Crist et al. 1981; Geisweid and Urbach 1983; Crist et al. 1988) and Cu by *P. syringae*

(Vasconcelos et al. 1997). However, this method has not been widely used for NMs and certainly not to evaluate the role of NM surface coatings on biosorption. In this study we accept the premise that the uptake of Cu NMs did not significantly change the external concentration in samples. For the highest tested concentration of pristine-CuO NMs suspension (71.33 µg L^{-1}), NH_3-CuO (24.16 µg L^{-1}), COOH-CuO (20.17 µg L^{-1}) and PEG-CuO (12.6 µg L^{-1}) 24h uptake efficiency was 0.24%, 0.28%, 0.17% and 0.56% respectively, indicating that just 0.172 µg L^{-1}, 0.068 µg L^{-1}, 0.0345 µg L^{-1} and 0.07 µg L^{-1} of Cu was biosorbed by 20 individuals after 24 hours. The estimated background amount of Cu in organisms c_b ranged between 7.478 and 63.02 µg g^{-1} for PEG-CuO NMs and pristine-CuO NMs exposures, respectively, and it was lower than 16% of maximum capacity *a*. A relatively high value of c_b (background) was observed because copper is a micronutrient and thus it is provided in the culture medium at a concentration of 4.19 µg l^{-1}.

Parameter *b* represents the relationship between changes in the external concentration and the amount of biosorbed Cu. The lower the *b* value the more acute the changes. In other words, low *b* values result in high biosorption even when the external concentration is relatively low. For example, the lowest value of the parameter *b* was observed for COOH-CuO NMs, 0.5931 µg l^{-1}, which indicates that for this relatively small concentration the values of 0.5 *a* parameter is already reached. The obtained *b* values can affect dose-response curves and are presented in Table 3.

The maximum capacity of Cu uptake (parameter *a*) was different for each tested NMs and $CuCl_2$. The obtained values of *a* [μg_{Cu} g^{-1}] can be ranked from the highest to lowest as follows:

316.1 (Pristine-CuO NMs) > 230 (NH_3-CuO NMs) > 157.1 (Aqueous Cu) > 87.66 (PEG-CuO NMs) > 66.27 (COOH-CuO NMs)

This configuration can be related to the physical and chemical properties of NMs and the organisms. The most important are mass, size, and electric charge. To compare the influence of mass on the maximum capacity of NMs we recalculated the estimated values of *a* and described it as a mass of whole NMs using calibration curves (Table 2). The

concentration of Cu in samples with $CuCl_2$ (aqueous Cu) was not recalculated because the salt dissociates to a very large extent and therefore only Cu ions should be considered to be biosorbed. After recalculation, the values of the parameter *a* were expressed in $\mu g_{nano}\ g^{-1}$ and can be ranked from the highest to lowest in the new configuration:

475.9 (NH_3-CuO NMs) >443.2 (Pristine-CuO NMs) > 347.7 (PEG-CuO NMs) > 164.3 (COOH-CuO NMs) > 157.1 (Aqueous Cu)

The first configuration shows how much Cu can be biosorbed by an organism when Cu is available in the different forms, the second shows how much of whole NMs can be biosorbed by the organism. In both cases, the highest uptake was observed for pristine-CuO and NH_3-CuO NMs and the lowest for PEG-CuO and COOH-CuO NMs. Cu ions should be classified according to the first configuration only. In general, it can be seen that the higher the accumulation of whole NMs, the higher the accumulation of Cu. The differences are caused by the various mass fractions of Cu in the different NMs (Table 1).According to the second configuration the maximum capacity of Cu ions was lower than obtained for all NMs. For ions the equilibrium was reached at a different point. It is likely that this is a result of the different chemical mechanisms (such as combination of van der Waals attraction and electrostatic repulsion between particles) affecting the behaviour of ions in homogenous solutions and NMs in suspension.

The electric charge could affect the mentioned configuration. The highest uptake was observed for the positively charged particles (NH_3-CuO and Pristine-CuO NMs), and the lowest for the negatively charged (COOH-CuO and PEG-CuO NMs). This could be related to the structure of an organism and, to the structure of cell membranes, as described below.

The negative charge of the carapace (zeta potential -14.5) can interact with the charge of NMs leading to increased biosorption for positively charged NMs or decreased for negatively charged NMs. However this hypothesis needs verification and further investigation.

It is also possible that negatively charged cell membranes (eg within the daphnia digestive tract) can interact with NMs in a similar manner as described above.

Furthermore, the charge of NMs can affect their transport across cell membranes and therefore toxicity. Intracellular Cu ion concentrations are regulated by many ATP-related active transport systems (Nies 1999). However, the transport of NMs is still in many cases unknown.

The charge of NMs is closely related with zeta potential in a certain medium (here M7). It is worth pointing out that the higher the zeta potential, the higher the maximum capacity of NMs in daphnids. Positive zeta potential values result in higher maximum capacity values compared to negative potential values. The highest zeta potential was 32.3 mV for NH_3-CuO NMs (a = 475.9 µg g^{-1}). The second highest value, 11.6 mV, was observed for pristine-CuO NMs and resulted in a maximum capacity value a = 443.2 µg g^{-1}. The difference in zeta potential for the two types of NMs results in a difference between values of the parameter a. Furthermore, NMs differed from each other in the mean agglomerate diameter (z-Average). The highest was found for NH_3-CuO NMs (350.23 nm) compared to the pristine-CuO NMs (286.76 nm). It was observed that higher values of z-Average (as well as zeta potential) were associated with higher a values when a was expressed as an amount of NMs. The way of expressing parameter a values is very important because different methods refer to completely different variables and lead to different conclusions, which can sometimes lead to misinterpretation of results (REF). Describing the amount of NMs seems to be more appropriate in this case rather than using amounts of Cu. This is because NMs with their specific physicochemical properties interact with organisms. The biosorbed Cu amount is strongly affected by the Cu mass fraction which can be different in each NM. The influence of Cu mass fraction can be clearly seen when comparing the two mentioned rankings, namely the higher amount of biosorbed NMs does not result in higher amount of Cu biosorbed.

The lowest zeta potential values were noted for COOH-CuO NMs (-14.8 mV) and PEG-CuO NMs (–15.5 mV) and these are associated with much lower maximum capacity values a compared to other NMs. The differences between the a values for COOH-CuO

and PEG-CuO NMs can result from differences in z-average (785.78 nm and 663.68 nm, respectively). In this case the higher z-Average the lower the *a* value. This suggests that the larger the size of negatively charged NMs the less likely biosorption to occur. For daphnids, the values of maximum capacity are higher for larger NMs clusters (as defined by DLS) with positive zeta potential and lower for larger NMs clusters with negative zeta potential. In summary, the higher the zeta potential of NMs the more biosorption is observed.

Each type of NMs has different biosorption properties. Furthermore, metal mass fraction in each of the tested NMs was different (m value, Table 2). Therefore, the amount of Cu inside the daphnids is the result of NMs physicochemical properties (such as their size, shape, zeta potential) and the Cu mass fraction which is carried by them. The differences between properties of the NMs result in the different configuration of maximum capacity. Nevertheless, it is likely that the Cu concentration is the main factor driving toxicity.

Probably only NMs which are suspended in the medium are available to, or at least directly interact with the daphnids in contrast to precipitated particles or those adsorbed to the walls of the vessels.

Kinetics of elimination

Another important aspect, which can provide key information on the interaction between organism and NMs is the rate and efficiency of elimination. Estimated model parameters are presented in Table 4 and Figure 2. The internal background Cu amount c_b when the elimination process reaches equilibrium (Table 4) was higher in all cases than c_b amount before exposure to NMs and $CuCl_2$, except for pristine-CuO NMs where the concentration after depuration was lower than before exposure. It is apparent that pristine-CuO NMs can likely be removed from organisms during depuration, which did not seem to be the case for the other NMs and the metal salt. Furthermore, there is a possibility that some NMs changed their chemical composition, by shedding ions or combining with chemicals in the medium, leading to incomplete depuration. This can explain the c_b values of NMs other than pristine-CuO, which probably is the most stable NM. The highest elimination rate k_e was observed for NH_3-CuO NMs (1.676 h^{-1}),

followed by the pristine-CuO NMs (1.435 h^{-1}). However, pristine-CuO NMs were removed completely compared to NH_3-CuO which indeed seem to yield increased internal amount after depuration (compared to the amount before biosorption). The lowest value of k_e was observed for COOH-CuO NMs. It can be suggested, supported by the results of equilibrium modeling (max. capacity *a*, Table 3), that these NMs are not capable of rapid migration between organism and water medium.

The elimination rate k_e was relatively high for Cu ions compared to NMs (1.382 h^{-1}). This could be related to mechanisms of Cu ion removal, which has an important role ensuring homeostasis in organisms. The amount of Cu inside living cells is regulated by different passive and active mechanisms (Nies 1999). For example, efflux of Cu driven by the proton gradient can be related to protein family RND (resistance, nodulation, cell division) which can consist of cell membrane proton/cation antiporter, membrane fusion protein, and some outer membrane factors (Nies 1999). The uptake of Cu ions takes place through membrane-integral proteins (MIT) due to the chemiosmotic gradient (Nies 1999). Active transport of Cu ions on both sides of the membrane is regulated by the P-type ATPases (Nies 1999). This system may be impaired by NMs which are not a natural part of the environment so the organisms may not have mechanisms to cope with them.

Correlation between biosorption, depuration processes and properties of NMs

Other correlations between model parameters were analyzed using linear Pearson coefficients. Results are given in Table 8. A high positive correlation was found between the maximum capacity value – parameter *a* (expressed as an amount of copper and whole NMs) and the rates of depuration process *v*. It indicates the mobility of NMs. Those NMs that are accumulated with high efficiency can be easily removed from the organism. The negative correlation between maximum capacity, parameter *b* values and agglomerate diameter (z-Average) show that smaller NMs have better biosorption properties. The correlation coefficients between zeta potential and values of *a* and *b* were higher than 0.8 and 0.66 respectively, indicating possible dependence between these values.

A high negative correlation was observed between the depuration constant k_e and agglomerate diameter (z-Average), and also maximum capacity (not with *b* parameter

values). It means that the depuration process is more intensive for smaller NMs which confirms previous observations.

A high positive correlation (> 0.5) between depuration parameter k_e and zeta potential was noted (Table 8), indicating that the zeta potential strongly affects the biosorption and depuration properties of NMs.

Results obtained show the large influence of the physicochemical properties of NMs on the biosorption and depuration of NMs, including their diameter and zeta potential.

Dose-response curves

Estimated parameters of the dose-response curve after 24 and 48 h are given in Tables 5 and 6 and in Figures 3 and 4. The coefficient of determination R^2 was higher than 0.9 for all samples except pristine-CuO and COOH-CuO NMs and, where it was found to be 0.8750 and 0.7795, respectively. However, SSE and RMSE values were acceptably low which indicates low values of errors between data and the fitted model (Tables 5 and 6).

Cu ions play an important role in living organisms (Harrison et al. 2000). They are well-known micronutrients and they are responsible for electron transport and oxygen transportation (Lodish et al. 2000; Ralph and McArdle 2001). However, above certain doses, they can be toxic (Santore et al. 2001; Di Toro et al. 2001).

A toxic effect was observed for all samples even at the lowest doses of NMs and this is described by the parameter *d* - lowest limit of effect (Tables 5 and 6). It denotes that for low values of internal dose, changes in toxic effects are small. Nevertheless, the toxic effect can still be observed. The highest *d* value was noted for pristine-CuO NMs (d = 0.2284 after 24h and d = 0.3769 after 48h). The value of the parameter *d* increases over time (24 - 48h), except for NH_3-CuO NMs where it decreases. It indicates the existence of a time dependent relationship between toxic effects and for the lowest NMs doses. The observed effect of low doses of Cu can be the result of different modes of toxic action of NMs and Cu ions. According to Biotic Ligand model predictions, accumulation associated with 50% mortality (LA50) has a value of 2.22 ng Cu/ g_{wet} (0.035 nmol Cu/g_{wet}) (Santore et al. 2001) which is lower than the value noted in our study (note the

lethal accumulation in Santore et al. (2001) is expressed per wet weight of the organism which can explain the difference between theirs and our study). NMs can cause similar effects as metal ions (when the ions are released from their structure by dissolution) or can act in a different manner and cause different effects due to their nanostructures. *d* – values were higher in pristine-CuO, COOH-CuO, PEG-CuO NMs after 48 h of exposition compared to 24h exposure. In the case of aqueous Cu only a low increase was observed, and in the case of NH_3-CuO NMs a small decrease was noted. These differences in low doses toxicity can be caused by the differences in physicochemical properties and molecular mechanisms of toxic action of Cu ions and NMs.

NMs and Cu ions doses lower than 50 µg g^{-1} for aqueous Cu; 180 µg g^{-1} for pristine-CuO NMs; 100 µg g^{-1} for NH3-CuO NMs; 70 µg g^{-1} for PEG-CuO NMs; 60 µg g^{-1} for COOH-CuO NMs cause small changes in toxicity. This can arguably be explained as a result of resistance (tolerance) of daphnids. After the dose exceeds a certain critical value the effect (toxicity) increases significantly (Figure 3 and 4/Table 5 and 6).

The increase in toxicity for the larger amount of biosorbed Cu (internal dose) is described by the slope of the dose-response curve – parameter *n*. Relatively low values of this parameter were observed for aqueous Cu, NH_3-CuO NMs and PEG-CuO NMs after 24h, and aqueous Cu, NH_3-CuO NMs after 48h of exposure. This shows that large changes in internal dose result in relatively small changes in toxic effects for these chemical substances. In contrast high values were observed for pristine-CuO NMs, COOH-CuO NMs after 24 and 48h and for PEG-CuO NMs after 48h. In this cases, after exceeding the critical value, the small changes in doses result in a very large change in toxicity. The differences between slopes of the dose-response curves could be affected by the chemical and physical properties of NMs and therefore related to characteristics of biosorption and depuration.

There were no significant linear correlations between *n* values and agglomerate diameter (z-Average), zeta potential and parameter *b* values (Table 8). However a strong negative correlation was observed between the *n* parameter and maximum capacity values (only when *a* was expressed as an amount of whole NMs per mass of organisms) and

elimination constant k_e. It means that higher depuration rate (so the mobility of NMs) and maximum capacity result in lower slopes of concentration-response curves. The changes in doses of mobile NMs caused predictable and slow changes in toxicity. For less mobile NMs (low *a* nad k_e) the effect changes rapidly in a small interval of internal doses.

Bozich et al. (2015) studied the effect of surface chemistry, charge and ligand type on Au NMs toxicity to *D. magna.* They reported that negatively charged Au NMs showed lower toxicity than positively charged Au NMs during short-term and chronic studies. Moreover in his study the crucial role of surface chemistry on NM toxicity was demonstrated. Nasser et al. (2016) demonstrated that the presence of the Au NMs positive charge attracted to a negative charge on the phospholipid membrane of the zooplankton leads to a decrease in toxicity in comparison to negatively charged NMs. Badawy et al. (2011) suggested that surface charge is one of the most important factors that govern the toxicity of NMs. Their results clearly demonstrate that the Ag NMs exhibited surface charge-dependent toxicity on the bacillus species investigated.

Our results demonstrate the crucial role NMs surface charges play on biosorption and depuration processes. Similarly, and as described above, negatively surface charged NMs were less available for daphnids, however surface charge was not correlated with acute toxicity. Pearson correlation coefficients between zeta potential and ED_{50} after 24 and 48 h (Table 7) were equal to 0.401 and 0.349 respectively - see Table 8. It should be pointed out that NMs with lower propensity to accumulate and to be removed from organisms were found to be more toxic.

Comparison between toxicities of NMs can be provided using parameter *e* values or calculated ED_{50}s (*e* and ED_{50} are not equal to each other as the lower limit of a function – parameter *d* is not equal to zero and was fitted to the data). NMs can be categorized from most to least toxic in the following configuration:

COOH-CuO NMs > PEG-CuO NMs > NH_3-CuO NMs > pristine-CuO NMs

for both 24 and 48 hours (Table 7). Aqueous Cu was less toxic than COOH-CuO NMs after 24 hours of exposure but more toxic after 48 hours. Cu ions act in a different way

than NMs. They do not follow the rules observed for NMs. They were most toxic (48h) and have relatively large maximum capacity value *a* and depuration constant value – which is opposite to what was observed for NMs.

A strong linear correlation was found between ED_{50}s (expressed as an amount of Cu) and *a* and *b* parameters values (also expressed as an amount of Cu). The lower the maximum capacity of NMs *a* and their properties to accumulate *b* the lower the ED_{50} values so toxicity is higher. It is apparent that higher biosorption capacity does not mean higher toxicity. Furthermore, high correlation between ED_{50}s and depuration parameters (k_e and *v*) was observed - the lower the mobility the higher the toxicity of NMs(lower ED_{50} values).The correlation between ED_{50}s and biosorption parameters (*a* and *b*) was much lower when parameter values were expressed as an amount of whole NMs. It is likely that permanent damage in organisms is caused by the metal fraction which is able to react with cell structures. This fraction depends on the chemical properties of NMs and could be called “effective metal fraction” of NMs. No correlations were observed between ED_{50} and NMs properties - agglomerate diameter (z-Average) and zeta potential (Table 8). It indicates that there is no simple or direct relationship between NMs properties and their toxicity.

CONCLUSIONS

In conclusion, the physical properties of whole NMs, including surface coating, affect the biosorption and depuration processes, however they are not directly correlated to NMs toxicity. The toxicity depends on available metal mass fraction and chemical composition of NMs. The biosorption process for different types of NMs was related to their physicochemical properties. Daphnids biosorbed larger and positively charged NMs more effectively. However, probably the electrostatic interaction between organism and NMs was weak; those NMs which were easily accumulated were also easily depurated. Those NMs with low maximum capacity values were difficult to depurate and were found to be more toxic.Copper ions act differently from NMs and they do not follow the rules observed for NMs. This could be a result of different properties affecting behaviour of ions in homogeneous solutions and NMs in suspension. Furthermore, biosorption and

removal of Cu ions could be related to the system ensuring homeostasis of organisms which may be impaired in relation to manufactured NMs which are not a natural part of environment.

Supplemental Data—The Supplemental Data are available on the Wiley Online Library at DOI: 10.1002/etc.xxxx.

Data accessibility—Data, associated metadata, and calculation tools are available from the corresponding author (z.gajda-meissner@hw.ac.uk).

References

Arambašić MB, Bjelić S, Subakov G. 1995. Acute toxicity of heavy metals (copper, lead, zinc), phenol and sodium on Allium cepa L., Lepidium sativum L. and Daphnia magna St.: Comparative investigations and the practical applications. Water Research. 29(2):497–503.

Aruoja V, Dubourguier H, Kasemets K, Kahru A. 2008. Toxicity of nanoparticles of CuO , ZnO and TiO 2 to microalgae Pseudokirchneriella subcapitata. Science of the Total Environment. 407(4):1461–1468. doi:10.1016/j.scitotenv.2008.10.053.

Badawy AMEL, Silva RG, Morris B, Scheckel KG, Suidan MT. 2011. Surface Charge-Dependent Toxicity of Silver Nanoparticles. Environmental Science & Technology. 45:283–287.

Benguella B, Benaissa H. 2002. Effects of competing cations on cadmium biosorption by chitin. Colloids and Surfaces. 201:143–150.

Bhattacharjee S. 2016. DLS and zeta potential - What they are and what they are not? Journal of Controlled Release. 235:337–351. doi:10.1016/j.jconrel.2016.06.017.

Bozich JS, Lohse SE, Torelli MD, Murphy CJ, Hamers RJ, Klaper RD. 2015. Surface chemistry, charge and ligand type impact the toxicity of gold nanoparticles to Daphnia magna. Environmental Science Nano. 1:260–270. doi:10.1039/c4en00006d.

Chen X, Mao SS. 2007. Titanium Dioxide Nanomaterials : Synthesis , Properties , Modifications , and Applications. Chemical Reviews. 107:2891–2959. doi:10.1021/cr0500535.

Cohen Y, Rallo R, Liu R, Liu HH. 2013. In Silico Analysis of Nanomaterials Hazard and Risk. Accounts of Chemical Research. 46(3):802–812. doi:10.1021/ar300049e.

Crist RH, Oberholser K, Schwartz D, Marzoff J, Ryder D, Crist DR. 1988. Interactions of

metals and protons with algae. Environmental Science & Technology. 22:755–760.

Crist RH, Oberholser K, Shank N, Nguyen M. 1981. Nature of bonding between metallic ions and algal cell walls. Environmental Science & Technology. 15:1212–1217.

Croteau MN, Misra SK, Luoma SN, Valsami-Jones E. 2014. Bioaccumulation and toxicity of CuO nanoparticles by a freshwater invertebrate after waterborne and dietborne exposures. Environmental Science and Technology. 48(18):10929–10937. doi:10.1021/es5018703.

Fomina M, Gadd GM. 2014. Bioresource Technology Biosorption : current perspectives on concept , definition and application. Bioresource Technology. 160:3–14. doi:10.1016/j.biortech.2013.12.102.

Fröhlich E. 2012. The role of surface charge in cellular uptake and cytotoxicity of medical nanoparticles. International Journal of Nanomedicine. 7:5577–5591. doi:10.2147/IJN.S36111.

Gadd GM. 1990. Heavy metal accumulation by bacteria and other microorganisms. Experientia. 46(8):834–840. doi:10.1007/BF01935534.

Geisweid HJ, Urbach W. 1983. Sorption of Cadmium by the Green Microalgae Chlorella vulgaris, Ankistrodesmus braunii and Eremosphaera viridis. Zeitschrift für Pflanzenphysiologie. 109(2):127–141.

Harrison MD, Jones CE, Solioz M, Dameron CT. 2000. Intracellular copper routing : the role of copper chaperones. Trends in Biochemical Sciences. 25(1):29–32.

Heinlaan M, Kahru A, Kasemets K, Arbeille B. 2011. Changes in the Daphnia magna midgut upon ingestion of copper oxide nanoparticles : A transmission electron microscopy study. Water Research. 45:179–190. doi:10.1016/j.watres.2010.08.026.

Jiang C, Aiken GR, Hsu-Kim H. 2015. Effects of Natural Organic Matter Properties on the Dissolution Kinetics of Zinc Oxide Nanoparticles. Environmental Science and Technology. 49(19):11476–11484. doi:10.1021/acs.est.5b02406.

Jiang C, Castellon BT, Matson CW, Aiken GR, Hsu-Kim H. 2017. Relative Contributions of Copper Oxide Nanoparticles and Dissolved Copper to Cu Uptake Kinetics of Gulf Killifish (Fundulus grandis) Embryos. Environmental Science and Technology. 51(3):1395–1404. doi:10.1021/acs.est.6b04672.

Jo HJ, Choi JW, Lee SH, Hong SW. 2012. Acute toxicity of Ag and CuO nanoparticle suspensions against Daphnia magna : The importance of their dissolved fraction varying with preparation methods. Journal of Hazardous Materials. 227–228:301–308. doi:10.1016/j.jhazmat.2012.05.066.

Kahru A, Dubourguier H. 2010. From ecotoxicology to nanoecotoxicology. Toxicology. 269(2–3):105–119. doi:10.1016/j.tox.2009.08.016.

Kalman J, Paul KB, Khan FR, Stone V, Fernandes TF. 2015. Characterisation of bioaccumulation dynamics of three differently coated silver nanoparticles and aqueous silver in a simple freshwater food chain. Environmental Chemistry. 12(6):662–672.

Khan FR, Paul KB, Dybowska AD, Valsami-Jones E, Lead JR, Stone V, Fernandes TF. 2015. Accumulation dynamics and acute toxicity of silver nanoparticles to daphnia magna and lumbriculus variegatus: Implications for metal modeling approaches. Environmental Science and Technology. 49(7):4389–4397. doi:10.1021/es506124x.

Liu J, Sonshine DA, Shervani S, Hurt RH. 2010. Controlled Release of Biologically Active Silver from Nanosilver Surfaces. ACS Nano. 4(11):6903–6913.

Lodish H, Berk A, Zipursky S, Al. E. 2000. Electron Transport and Oxidative Phosphorylation. In: Molecular Cell Biology. 4th editio. New York: W. H. Freeman.

Misra SK, Dybowska A, Berhanu D, Luoma SN, Valsami-Jones E. 2012. The complexity of nanoparticle dissolution and its importance in nanotoxicological studies. Science of the Total Environment. 438:225–232. doi:10.1016/j.scitotenv.2012.08.066.

Nasser F, Davis A, Valsami-Jones E, Lynch I. 2016. Shape and Charge of Gold Nanomaterials Influence Survivorship , Oxidative Stress and Moulting of Daphnia magna. Nanomaterials. 6(12):2–13. doi:10.3390/nano6120222.

Nies DH. 1999. Microbial heavy-metal resistance. Applied Microbiology and Biotechnology. 51:730–750.

Nolte TM, Hartmann NB, Kleijn JM, Garnæs J, Meent D Van De, Hendriks AJ, Baun A. 2017. The toxicity of plastic nanoparticles to green algae as influenced by surface modification , medium hardness and cellular adsorption. Aquatic Toxicology. 183:11–20. doi:10.1016/j.aquatox.2016.12.005.

Palza H, Nuñez M, Bastías R, Delgado K. 2018. International Journal of Antimicrobial Agents In situ antimicrobial behavior of materials with copper-based additives in a hospital environment. International Journal of Antimicrobial Agents. 51(6):912–917. doi:10.1016/j.ijantimicag.2018.02.007.

Pane EF, McGeer JW, Wood CM. 2004. Effects of chronic waterborne nickel exposure on two successive generations of Daphnia magna. Environmental Toxicology and Chemistry. 23(4):1051–1056.

Ralph A, McArdle HJ. 2001. Copper Metabolism and Requirements in the Pregnant Mother, Her Fetus, and Children. New York: International Copper Association.

Ren G, Hu D, Cheng EWC, Vargas-reus MA, Reip P, Allaker RP. 2009. Characterisation of copper oxide nanoparticles for antimicrobial applications. International Journal of Antimicrobial Agents. 33:587–590. doi:10.1016/j.ijantimicag.2008.12.004.

Robinson KA, Baird DJ, Wrona FJ. 2003. Surface metal adsorption on zooplankton carapaces : implications for exposure and effects in consumer organisms. Environmental Pollution. 122:159–167.

Santore RC, Di Toro DM, Paquin PR, Allen HE, Meyer JS. 2001. Biotic ligand model of the acute toxicity of metals. 2. Application to acute copper toxicity in freshwater fish and daphnia. Environmental Toxicology and Chemistry. 20(10):2397–2402.

Di Toro DM, Allen HE, Bergman HL, Meyer JS, Paquin PR, Santore RC. 2001. Biotic ligand model of the acute toxicity of metals. 1. Technical basis. Environmental Toxicology and Chemistry. 20(10):2383–2396.

Vasconcelos MTSD, Azenha MAO, Cabral JPS. 1997. Comparison of availability of copper(II) complexes with organic ligands to bacterial cells and to chitin. Environmental Chemistry. 16(10):2029–2039.

Veglio F, Beolchini F. 1997. Removal of metals by biosorption: a review. Hydrometallurgy. 44(3):301–316. doi:10.1016/S0304-386X(96)00059-X.

Wang J, Chen C. 2009. Biosorbents for heavy metals removal and their future. Biotechnology Advances. 27(2):195–226. doi:10.1016/j.biotechadv.2008.11.002.

Winkler DA. 2016. Recent advances , and unresolved issues , in the application of computational modelling to the prediction of the biological effects of nanomaterials. Toxicology and Applied Pharmacology. 299:96–100. doi:10.1016/j.taap.2015.12.016.

Xu G, Huo D, Hou C, Zhao Y, Bao J, Yang M, Fa H. 2018. A regenerative and selective electrochemical aptasensor based on copper oxide nano fl owers-single walled carbon nanotubes nanocomposite for chlorpyrifos detection. Talanta. 178(August 2017):1046–1052. doi:10.1016/j.talanta.2017.08.086.

Figures

Fig. 1. Langmuir curves for copper ions and different NMs; black dots indicates experimental data, solid line indicates fitted model; dotted line indicates prediction intervals

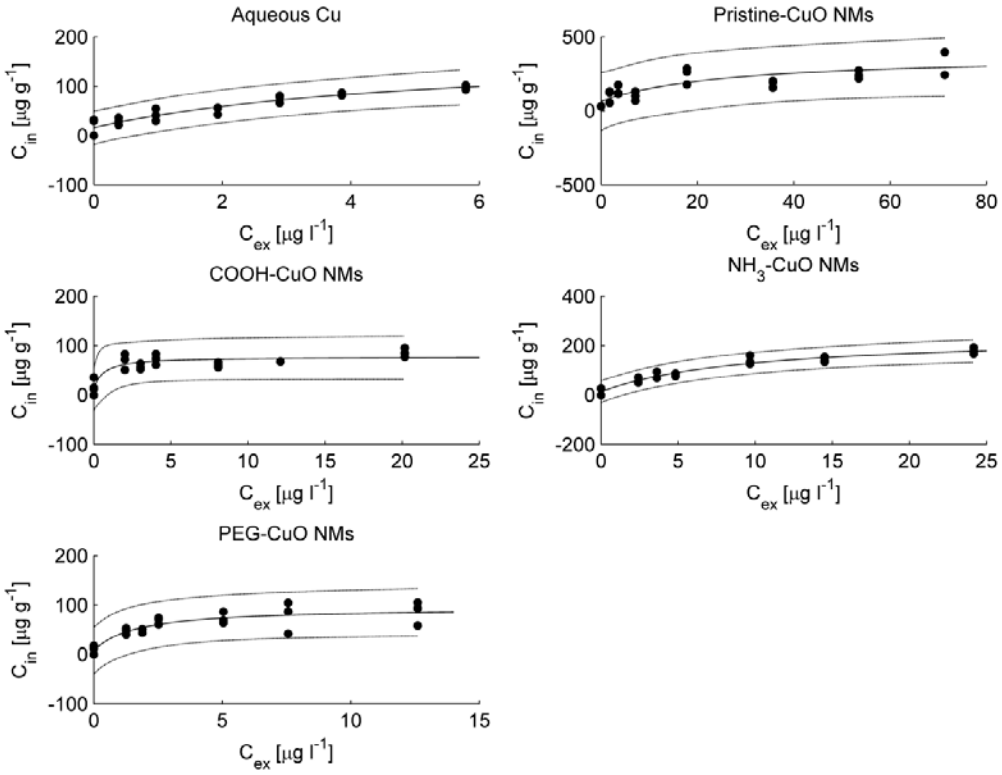

Fig. 2. Depuration kinetics for copper ions and different NMs; black dots indicates experimental data, solid line indicates fitted model; dotted line indicates prediction intervals

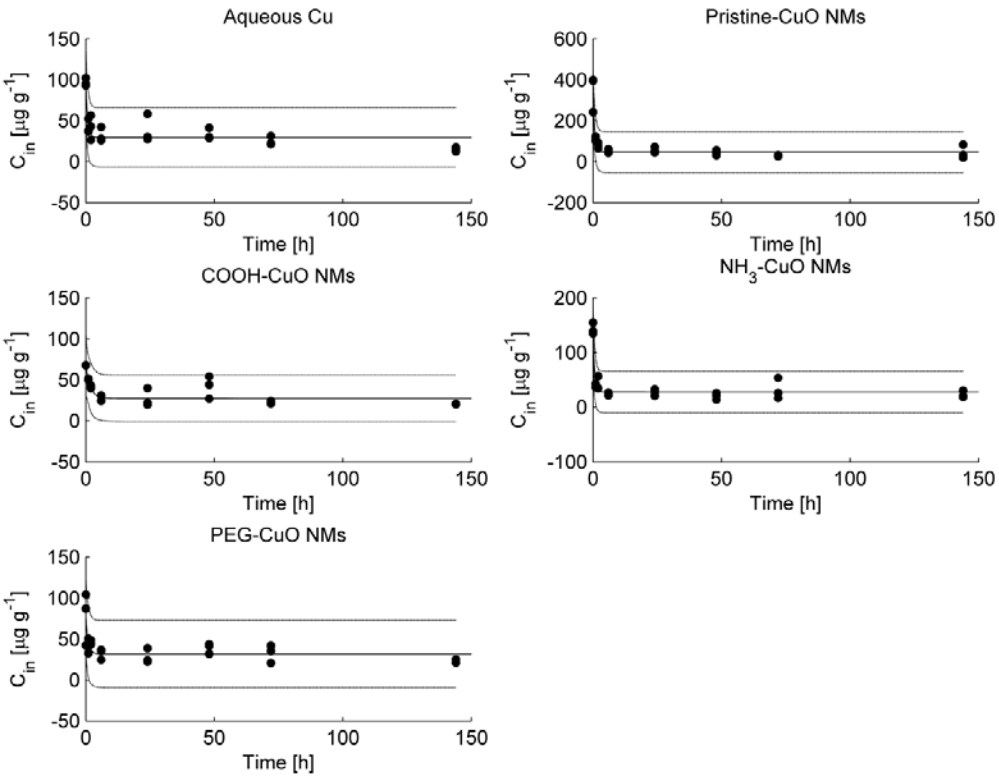

Fig. 3. Dose-response curves for copper ions and different NMs after **24h** of exposition; black dots indicates experimental data, solid line indicates fitted model; dotted line indicates prediction intervals

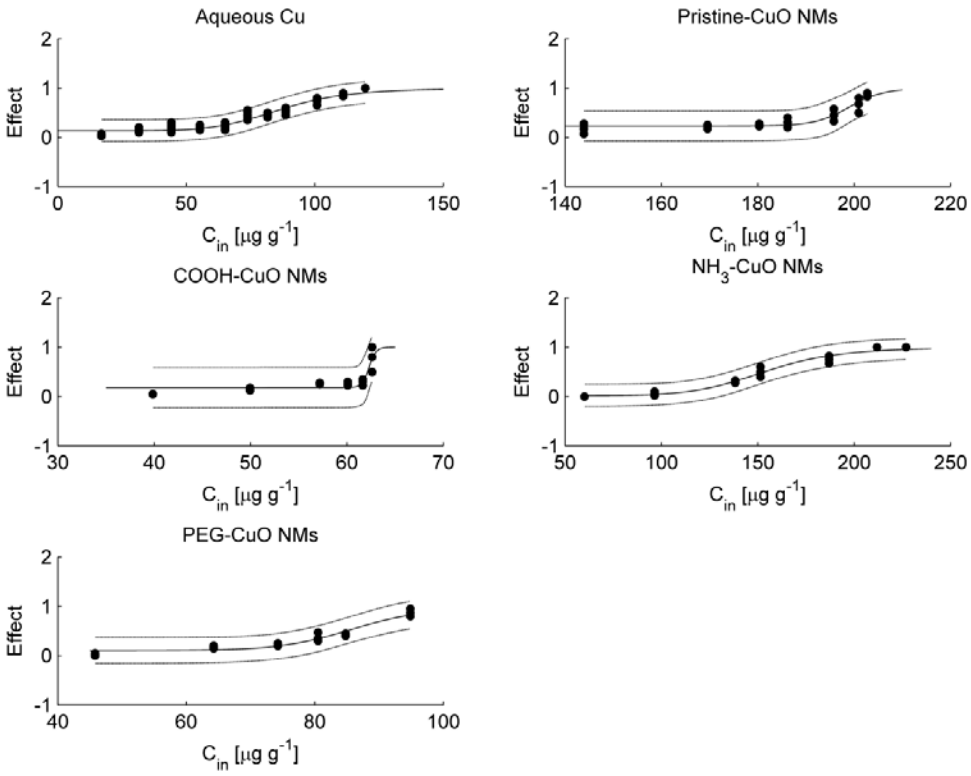

Fig. 4. Dose-response curves for copper ions and different NMs after **48h** of exposition; black dots indicates experimental data, solid line indicates fitted model; dotted line indicates prediction intervals

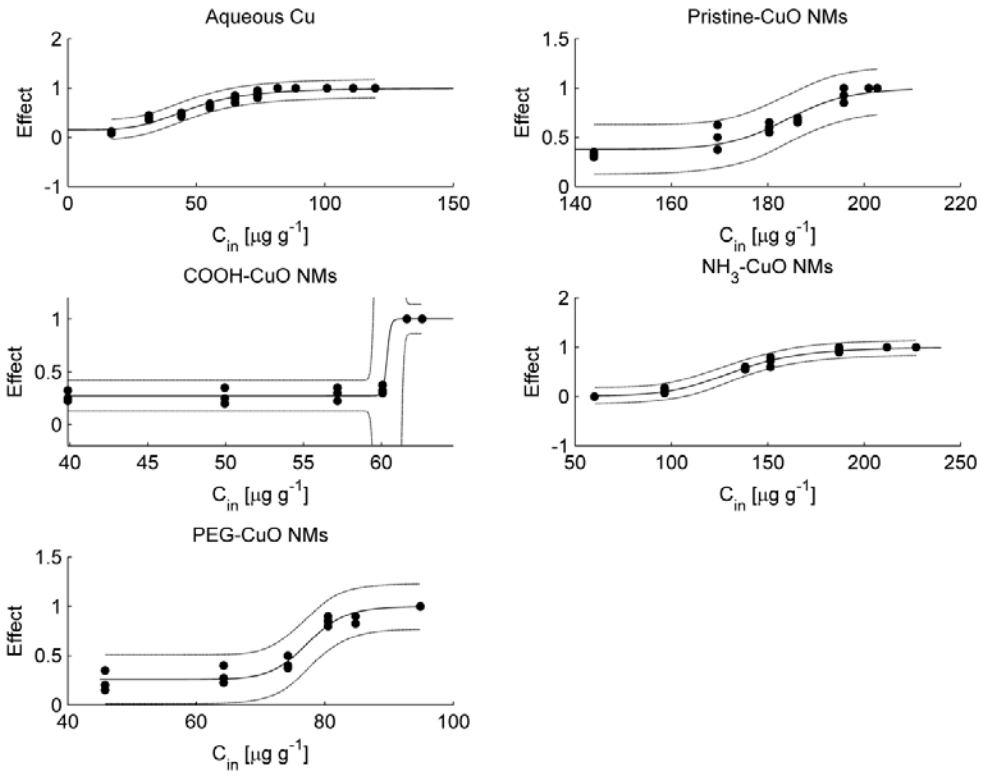

Table 1. NMs properties - diameter (z-Average), polydispersity index (PDI) ± standard deviation, zeta potential values and the fraction of dissolved copper

Sample	z-Average [nm]	PDI	Zeta potential [mV]	**fraction of dissolved Cu**
Pristine-CuO NMs	286.76 ±29.95	0.408 ±0.053	11.6	0.05
COOH-CuO NMs	785.78 ±191.80	0.559 ±0.099	-14.8	0.85
NH_3-CuO NMs	350.23 ±25	0.512 ±0.13	32.3	0.35

PEG-CuO NMs	663.68 ±126.58	0.582 ±0.224	-15.5	0.86
$CuCl_2$	-	-	-	0.95

Table 2. ***The mass fraction of copper in NMs***

	Parameter (with 95% confidence bounds)	Goodness of fit			
	m	SSE	R^2	Adj. R^2	RMSE
Aqueous Cu	0.386 (0.3844, 0.3877)	0.2002	0.9999	0.9999	0.1292
Pristine-CuO NMs	0.7133 (0.6816, 0.7449)	76.7872	0.9932	0.9932	2.5296
COOH-CuO NMs	0.4034 (0.3987, 0.4082)	1.7509	0.9995	0.9995	0.3820
NH_3-CuO NMs	0.4833 (0.4821, 0.4846)	0.1198	1.0000	1.0000	0.0999
PEG-CuO NMs	0.2521 (0.2453, 0.259)	2.5005	0.9980	0.9980	0.5271

SSE - sum squared error; R^2 - coefficient of determination (unadjusted); Adj. R^2 - adjusted for the number of coefficients; RMSE - root mean squared error;

Table 3. Estimated parameter values of Langmuir model.

	Parameters (with 95% confidence bounds)			Goodness of fit			
	a [µg g^{-1}]	b [µg l^{-1}]	c_b [µg g^{-1}]	SSE	R^2	Adj. R^2	RMSE
Aqueous Cu	157.1 (67.4, 246.7)	5.252 (-0.3773, 10.88)	15.78 (7.745, 23.81)	2.2949e+003	0.8999	0.8903	10.4538
Pristine-CuO NMs	316.1 (143, 489.1)	26.18 (-19.48, 71.83)	63.02 (9.293, 116.7)	7.3946e+004	0.7013	0.6728	59.3401
COOH-CuO NMs	66.27 (48.07, 84.47)	0.5931 (-0.4321, 1.618)	10.6 (-0.5961, 21.8)	3.2628e+003	0.8236	0.8051	13.1045
NH_3-CuO NMs	230 (187.9, 272.2)	9.629 (5.06, 14.2)	13.06 (1.85, 24.28)	3.8583e+003	0.9526	0.9481	13.5547
PEG-CuO NMs	87.66 (64.03, 111.3)	1.624 (0.1642, 3.084)	7.478 (-4.903, 19.86)	4.4923e+003	0.8109	0.7929	14.6260

Table 4. Estimated parameter values of kinetic model.

	Parameters (with 95% confidence bounds)			Goodness of fit			
	C_{in0} [µg g^{-1}]	k_e [h^{-1}]	c_b [µg g^{-1}]	SSE	R^2	Adj. R^2	RMSE
Aqueous Cu	66.5 (51.38, 81.61)	1.382 (0.533, 2.23)	29.65 (23.56, 35.74)	2.8283e+003	0.7997	0.7806	11.6052
Pristine-CuO NMs	297.8 (256.1, 339.5)	1.435 (0.8792, 1.992)	46.32 (29.56, 63.09)	2.1552e+004	0.9130	0.9047	32.0355
COOH-CuO NMs	40.57 (22.92, 58.22)	0.5764 (0.1199, 1.033)	27.56 (22.54, 32.58)	1.5043e+003	0.6390	0.6010	8.8980
NH_3-CuO NMs	114.3 (98.42, 130.2)	1.676 (0.8364, 2.516)	27.87 (21.54, 34.19)	2.9562e+003	0.9184	0.9103	12.1577
PEG-CuO NMs	45.23 (28.22, 62.25)	1.063 (0.1009, 2.025)	31.65 (24.67, 38.63)	3.5997e+003	0.5959	0.5574	13.0925

Where: SSE - sum squared error; R^2 - coefficient of determination (unadjusted); Adj. R^2 - adjusted for the number of coefficients; RMSE - root mean squared error;

Table 5. Estimated parameter values of internal dose -response curve (24h).

	Parameters (with 95% confidence bounds)			Goodness of fit			
	n	d	e	SSE	R^2	Adj. R^2	RMSE
Aqueous Cu	6.5 (5.372, 7.628)	0.1338 (0.09672, 0.1709)	86.88 (84.27, 89.5)	0.2861	0.9440	0.9418	0.0742
Pristine-CuO NMs	55.56 (26.48, 84.64)	0.2284 (0.1665, 0.2903)	199 (197.3, 200.7)	0.1633	0.8750	0.8612	0.0952
COOH-CuO NMs	173.6 (53.23, 294.1)	0.1802 (0.1029, 0.2575)	62.29 (61.98, 62.6)	0.2328	0.7795	0.7502	0.1246
NH_3-CuO NMs	7.973 (6.09, 9.857)	0.0212 (-0.04055, 0.08296)	154.2 (148.9, 159.5)	0.0794	0.9748	0.9720	0.0664
PEG-CuO NMs	14.72 (9.66, 19.77)	0.1041 (0.03448, 0.1737)	86.21 (84.09, 88.34)	0.0912	0.9316	0.9225	0.0780

Table 6. Estimated parameter values of internal dose -response curve (48h).

	Parameters (with 95% confidence bounds)			Goodness of fit			
	n	d	e	SSE	R^2	Adj. R^2	RMSE
Aqueous Cu	4.149 (3.445, 4.853)	0.1528 (0.09224, 0.2134)	47.73 (44.69, 50.77)	0.2152	0.9557	0.9540	0.0643
Pristine-CuO NMs	28.84 (17.32, 40.36)	0.3769 (0.2984, 0.4554)	184.3 (181, 187.5)	0.0960	0.9267	0.9185	0.0730
COOH-CuO NMs	510.4 (-1.273e+005, 1.283e+005)	0.275 (0.2437, 0.3063)	60.36 (-11.31, 132)	0.0292	0.9858	0.9839	0.0441
NH_3-CuO NMs	7.428 (5.703, 9.152)	0.01699 (-0.03792, 0.07189)	133.1 (128.1, 138)	0.0413	0.9869	0.9854	0.0479
PEG-CuO NMs	26.39 (16.41, 36.38)	0.2593 (0.1934, 0.3251)	77.39 (75.91, 78.88)	0.0803	0.9531	0.9468	0.0732

Where: SSE - sum squared error; R^2 - coefficient of determination (unadjusted); Adj. R^2 - adjusted for the number of coefficients; RMSE - root mean squared error;

Table 7. ED_{50}s for different types of NMs and copper ions after 24 and 48h of exposure

	ED_{50} 24h [$\mu g_{Cu}\ g^{-1}$]	ED_{50} 48h [$\mu g_{Cu}\ g^{-1}$]
Aqueous Cu	82.82	43.71
Pristine-CuO NMs	196.83	175.56
COOH-CuO NMs	62.13	60.27
NH_3-CuO NMs	153.36	132.48
PEG-CuO NMs	84.85	75.28

Tab. 8. Pearson correlation coefficients (n.c. – not calculated)

	a [$\mu g_{Cu}\ g^{-1}$]	a [$\mu g_{nano}\ g^{-1}$]	b [$\mu g_{Cu}\ l^{-1}$]	b [$\mu g_{nano}\ l^{-1}$]	k_e [h^{-1}]	n (24h)	n (48h)	ED_{50} (24h) [$\mu g_{Cu}\ g^{-1}$]	ED_{50} (48h) [$\mu g_{Cu}\ g^{-1}$]	ED_{50} (24h) [$\mu g_{nano}\ g^{-1}$]	ED_{50} (48h) [$\mu g_{nano}\ g^{-1}$]	z-Average [nm]	Zeta [mV]
a [$\mu g_{Cu}\ g^{-1}$]	1	n.c.	n.c.	n.c.	0.814	-0.435	-0.611	0.997	0.998	n.c.	n.c.	n.c.	n.c.
a [$\mu g_{nano}\ g^{-1}$]		1	n.c.	n.c.	0.986	-0.871	-0.930	n.c.	n.c.	0.810	0.783	-0.917	0.809
b [$\mu g_{Cu}\ l^{-1}$]			1	n.c.	0.624	-0.270	-0.492	0.945	0.961	n.c.	n.c.	n.c.	n.c.
b [$\mu g_{nano}\ l^{-1}$]				1	0.755	-0.41	-0.61	n.c.	n.c.	0.350	0.328	-0.94	0.668

^{1}]						8	4					0	
k_e [h^{-1}]					1	-0.819	-0.865	0.842	0.810	0.740	0.705	-0.926	0.895
n (24h)						1	n.c.	n.c.	n.c.	n.c.	n.c.	0.604	-0.519
n (48h)							1	n.c.	n.c.	n.c.	n.c.	0.737	-0.552
ED_{50} (24h) [$\mu g_{Cu}\ g^{-1}$]								1	n.c.	n.c.	n.c.	n.c.	n.c.
ED_{50} (48h) [$\mu g_{Cu}\ g^{-1}$]									1	n.c.	n.c.	n.c.	n.c.
ED_{50} (24h) [$\mu g_{nano}\ g^{-1}$]										1	n.c.	-0.517	0.401
ED_{50} (48h) [$\mu g_{nano}\ g^{-1}$]											1	-0.484	0.349
z-Average												1	n.c.

[nm]													
Zeta [mV]													1